0090-9556/00/2804-0446–459$02.00/0
DRUG METABOLISM AND DISPOSITION
Vol. 28, No. 4
Printed in U.S.A.

METABOLISM AND DISPOSITION OF MOXONIDINE IN FISCHER 344 RATS

MINXIA M. HE, TRENT L. ABRAHAM, THOMAS J. LINDSAY, SYLVIA H. CHAY, BORIS A. CZESKIS, AND LISA A. SHIPLEY

Department of Drug Metabolism and Disposition, Lilly Research Laboratories, Eli Lilly and Company, Lilly Corporate Center, Indianapolis, Indiana

(Received August 20, 1999; accepted December 17, 1999)

This paper is available online at http://www.dmd.org

ABSTRACT:

The metabolism and disposition of moxonidine (4-chloro-5-(imidazolidin-2-ylidenimino)-6-methoxy-2-methylpyrimidine), a potent central-acting antihypertensive agent, were investigated in F344 rats. After an i.v. or oral administration of 0.3 mg/kg of [^{14}C]moxonidine, the maximum plasma concentrations of moxonidine were determined to be 146.0 and 4.0 ng/ml, respectively, and the elimination half-lives were 0.9 and 1.1 h, respectively. The oral bioavailability of moxonidine was determined to be 5.1%. The metabolic and elimination profiles of moxonidine were determined after an oral administration of 5 mg/kg of [^{14}C]moxonidine. More than fifteen phase I and phase II metabolites of moxonidine were identified in the different biological matrices (urine, plasma, and bile). Oxidative metabolism of moxonidine leads to the formation of hydroxymethyl moxonidine and a carboxylic acid metabolite as the major metabolites. Several GSH conjugates, cysteinylglycine conjugates, cysteine conjugates, and a glucuronide conjugate were also identified in rat bile samples. The radiocarbon was eliminated primarily by urinary excretion in rats, with 59.5% of total radioactivity recovered in the urine and 38.4% recovered in the feces within 120 h. In bile duct-cannulated rats, about 39.7% of the radiolabeled dose was excreted in the urine, 32.6% excreted in the bile, and approximately 2% remained in the feces. The results from a quantitative whole body autoradiography study indicate that radiocarbon associated with [^{14}C]moxonidine and/or its metabolites was widely distributed to tissues, with the highest levels of radioactivity observed in the kidney and liver. In summary, moxonidine is well absorbed, extensively metabolized, widely distributed into tissues, and rapidly eliminated in rats after oral administration.

Moxonidine (4-chloro-5-(imidazolidin-2-ylidenimino)-6-methoxy-2-methylpyrimidine), is a representative of a new class of central acting antihypertensive drugs. It is believed to act on central nervous system imidazoline receptors to decrease sympathetic nervous system tone (Ernsberger et al., 1992). Moxonidine is a potent and effective agent for the treatment of hypertension in Europe, with daily administered doses of 0.2 to 0.4 mg. It is also well tolerated in patients (Ollivier et al., 1992). When compared with clonidine and rilmenidine, moxonidine has fewer adverse drug effects, such as dry mouth and sedation, because it is considerably more selective for the I_1 receptor than the α_2 receptor that is associated with those side effects (Yu and Frishman, 1996). The chemical structure of moxonidine is shown in Fig. 1. Although moxonidine has been used for treatment of hypertension for a few years, the metabolism and disposition of the drug were not fully characterized in animal species due to limited technology available at the time when the compound was originally developed.

In this study, the metabolism and disposition of moxonidine were investigated in Fischer 344 rats. Plasma pharmacokinetics was determined after oral and i.v. administration of ^{14}C-radiolabeled moxonidine. The biotransformation of moxonidine was characterized after oral administration of [^{14}C]moxonidine. The metabolites were identified in the different biological matrices (urine, plasma, and bile) using HPLC with radiochemical detection, liquid chromatography-mass spectrometry (LC/MS)[1], and tandem mass spectrometry (LC/MS/MS). The elimination of radiocarbon after an oral dose of ^{14}C-radiolabeled moxonidine was determined in both noncannulated and bile duct-cannulated rats. The tissue distribution of moxonidine in F344 rats was also determined by quantitative whole body autoradiography (QWBA).

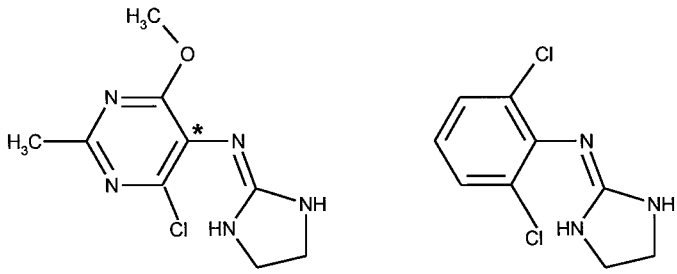

Moxonidine Clonidine

FIG. 1. *Chemical structures of moxonidine and clonidine (internal standard).*
*, Indicates position of ^{14}C-radiolabel.

Send reprint requests to: Dr. Minxia M. He, Department of Drug Metabolism and Disposition, DC 0710, Lilly Research Laboratories, Eli Lilly and Company, Lilly Corporate Center, Indianapolis, IN 46285. E-mail: He_Michelle_Minxia@Lilly.Com

[1] Abbreviations used are: LC/MS, liquid chromatography-mass spectrometry; QWBA, quantitative whole body autoradiography; LC/MS/MS, tandem mass spectrometry; GST, glutathione *S*-transferase; GC/MS, gas chromatography/mass spectrometry; C_{max}, peak plasma concentration; T_{max}, time to reach C_{max}; AUC, area under the plasma concentration time curve; BQL, below the quantitation limit; TCA, trichloroacetic acid.

Experimental Procedures

Chemicals and Materials. Unlabeled moxonidine with a purity of 99.9% (HPLC) was synthesized at Lilly Research Laboratories. [^{14}C]Moxonidine was synthesized by the radiochemistry group at the Department of Drug Disposition, Lilly Research Laboratories. The radiochemical purity of [^{14}C]moxonidine was 98.9% (thin layer chromatography-autoradiography) or 98.6% (radio-HPLC), and the specific activity was 81.89 μCi/mg. Moxonidine metabolites (dehydrogenated moxonidine, hydroxymethyl moxonidine, carboxylic acid metabolite, guanidine metabolite, and cysteine conjugate) were synthesized by the radiochemistry group and chemistry group at Lilly Research Laboratories. HPLC grade acetonitrile and methanol and analytical reagent grade potassium hydroxide, hydrogen peroxide, and glacial acetic acid were purchased from Mallinkrodt Baker, Inc. (Paris, KY). SDS was purchased from Bio-Rad Laboratories (Richmond, CA). Denatured ethanol (190 proof) was purchased from AAPER Alcohol and Chemical Company (Shelbyville, KY). Ammonium acetate and sodium phosphate were purchased from J. T. Baker (Phillipsburg, NJ). Trichloroacetic acid (TCA) was purchased from Fisher Scientific (Fairlawn, NJ). NADPH, GSH, rat glutathione *S*-transferase (GST) and carboxymethylcellulose were purchased from Sigma Chemical Co. (St. Louis, MO). Ultima Gold XR Cocktail was purchased from Packard (Meriden, CT). Beckman Ready scintillant was purchased from Beckman Instruments (Fullerton, CA). Cryomicrotome was purchased from Leica (Deerfield, IL). Milli-Q was purchased from Millipore Corp. (Bedford, MA). LC-ABZ columns obtained from Supelco, Inc. (Bellefonte, PA) were used for chromatography. Fischer 344 rats were obtained from Harlan Sprague-Dawley, Indianapolis, IN.

Pharmacokinetics. *Sample collection.* Pharmacokinetic studies were conducted in male F344 rats after an i.v. or oral dose of 0.3 mg/kg of [^{14}C]moxonidine (radioactive dose of 18.9 μCi/kg for i.v., or 23.6 μCi/kg for oral). The i.v. study was performed using a staggered design with one rat per time point. All animals were fasted overnight before dosing and fed 4 h after dosing. Whole blood was collected in heparinized vacutainer tubes via cardiac puncture at 0.083, 0.166, 0.25, 0.333, 0.5, 0.75, 1, 1.5, 2, 3, 4, 5, 6, 8, 10, 12, 16, 24, 36, and 48 h after dosing. In the oral study, moxonidine was given to four rats for each time point. Whole blood was collected in heparinized vacutainer tubes via cardiac puncture at 0.25, 0.5, 1, 2, 4, 6, 8, 12, 24, and 48 h after dosing. For both i.v. and oral studies, plasma samples were prepared by centrifugation of the whole blood. The plasma samples were stored at approximately −70°C before analyses.

Determination of radioequivalents. Radioequivalents of [^{14}C]moxonidine in whole blood and plasma were determined by liquid scintillation counting using an external standard to measure the efficiency of counting via a channel ratio method. Three aliquots of whole blood (100 μl) were placed into combustion thimbles. The samples were allowed to dry and then combusted in a Packard Tricarb Oxidizer 307. The resulting $^{14}CO_2$ was trapped and counted for radioactivity by a Packard Tricarb liquid scintillation analyzer 1600 TR. Three aliquots of plasma (100 μl) were transferred to individual scintillation vials, and samples were mixed with 10 ml of Beckman Ready scintillant and counted by the Packard Tricarb liquid scintillation analyzer.

Determination of moxonidine concentrations by gas chromatography/mass spectrometry (GC/MS). Plasma samples were analyzed at Oneida Research Services, Inc., using a GC/MS method. Aliquots of rat plasma (0.5 ml) were fortified with 250 pg of internal standard (clonidine HCl). Each sample was extracted into ethyl acetate under basic conditions, the organic layer was removed, and the plasma discarded. Samples were back extracted with 0.5 M HCl and the organic layer was discarded. Samples were then extracted into methylene chloride under basic conditions, the aqueous layer discarded, and the organic layer was dried under a stream of nitrogen. After evaporation, samples were derivatized with 3, 5-bis-(trifluoromethyl)-benzoyl chloride and again evaporated under nitrogen. After evaporation, samples were reconstituted in 50 μl of acetonitrile, transferred to autosampler vials, and 1 to 2 μl was injected onto the GC/MS system. GC/MS was performed on a Hewlett-Packard 5890A with a 10 M DB-17 (0.25 mm, 0.25 μm coating) capillary column interfaced with a Finnigan TSQ-45 mass spectrometer. The mass spectrometry was performed in selected ion monitoring mode, using negative ion methane chemical ionization. Moxonidine concentrations were determined by monitoring ions at *m*/*z* 685 (for moxonidine) and *m*/*z* 673 (for clonidine). The method was evaluated from the concentration range of 0.050 to 10 ng/ml. Plasma samples with concentrations of moxonidine above 10 ng/ml were diluted with blank plasma and reanalyzed.

PK data analysis. Pharmacokinetic parameters including peak plasma concentration (C_{max}), time to reach C_{max} (T_{max}), area under the plasma concentration time curve (AUC), initial elimination half-life ($T_{1/2(\alpha)}$), terminal elimination half-life ($T_{1/2(\beta)}$) were calculated using noncompartmental methods in the Eli Lilly and Company ADME/PTK computer software application.

Calculations of pharmacokinetic parameters for moxonidine. Samples below the quantitation limit (BQL) of 0.050 ng/ml were assigned a value of zero. For the i.v. study, the concentration of moxonidine at 0 h was obtained by extrapolation based on the 0.083-, 0.166-, 0.25-, and 0.333-h concentration values. For the oral study, the concentration of moxonidine at 0 h was assigned a value of zero for AUC calculation purpose. AUC_{0-6h} was calculated for both i.v. and oral studies to determine the bioavailability of moxonidine.

Calculations of pharmacokinetic parameters for plasma and blood radioactivity. In the i.v. study, samples BQL of 1.1 and 0.8 ng-Eq./ml were assigned a value of zero for calculations of pharmacokinetic parameters for plasma radioactivity and whole blood radioactivity, respectively. In the oral study, samples BQL of 0.9 and 0.7 ng-Eq/ml were assigned a value of zero for calculations of pharmacokinetic parameters for plasma radioactivity and whole blood radioactivity, respectively. The minimum detectable radioactivity was calculated based on background counts per minute, counting time, and the specific activity of the dose.

Metabolite Identification. *Sample preparation.* Urine samples collected at 0 to 12 or 12 to 24 h post dose from a balance excretion study (described below) were centrifuged, and the supernatant was injected directly onto HPLC for metabolite profiling. For LC/MS/MS analysis, urine samples were diluted 1:1 with 25 mM ammonium acetate buffer (pH 5.0) before injection. Rat bile samples collected at 0 to 8 and 8 to 16 h post dose from bile duct-cannulated rats in a biliary excretion study (also described below) were used for identification of biliary metabolites. The bile samples were diluted 1:1 with 25 mM ammonium acetate (pH 5.0) before analyses by LC/MS/MS. Plasma samples used for metabolite identification were obtained from a separate study in which animals were dosed with 5 mg/kg of [^{14}C]moxonidine. Blood was collected at 1, 2, and 4 h post dose. Plasma samples at each time point were pooled and prepared as follows: Two milliliters of each plasma sample analyzed was mixed with 340 μl of 20% TCA to precipitate plasma proteins. The samples were then centrifuged at approximately 3800 rpm for approximately 5 min to pellet the precipitated proteins. The entire volume of the supernatant fraction of the sample was transferred to a Varian C18, 200-mg, 3-ml solid-phase extraction cartridge, which had been conditioned with 2 ml of methanol and equilibrated with 2 ml of 1% TCA. The cartridge was then rinsed with 2 ml of 1% TCA, and moxonidine-related substances were eluted with 2 ml of 25 mM ammonium acetate (pH 5.0):acetonitrile (50:50). The effluent was evaporated to dryness at approximately 37°C under nitrogen. Samples were reconstituted in 250 μl of 25 mM ammonium acetate buffer (pH 5.0) before analyses by LC/MS/MS.

HPLC profiling of metabolites. Determination of urinary metabolites was performed using a Waters 600 MS system, equipped with a reversed phase C18 Supelcosil LC-ABZ column (25 cm × 4.6 mm, 5 μm) and a Ramona-92 radiochemical detector with a 100-μl solid flow cell. The metabolites and moxonidine were separated by a gradient elution at a flow rate of 1 ml/min. A mobile phase gradient of 50 mM ammonium acetate (pH 5.0) (A) and acetonitrile (B) was programmed as follows: started with 100% solvent A; changed to solvent A/solvent B at 95:5 over 0 to 20 min; held at 95:5 from 20 to 35 min.

LC/MS and LC/MS/MS. Separation was performed using a C18 Supelcosil LC-ABZ column (25 cm × 4.6 mm, 5 μm) at a flow rate of 1 ml/min (Waters 600 MS pump). The flow was split to allow 250 μl to flow into the electrospray source and 750 μl to a Ramona 5-LS radiochemical detector with a solid flow cell, which provided simultaneous detection of radioactivity and mass spectrometry. A mobile phase gradient of 25 mM ammonium acetate (pH 5) (A) and acetonitrile (B) was programmed as follows: started with 100% solvent A; changed to solvent A/solvent B at 95:5 over 0 to 20 min; held at 95:5 from 20 to 25 min; changed to 100% solvent A from 25 to 26 min. The gradient was changed slightly to optimize the separation for each matrix. The characterization of the metabolites was performed on a Finnigan TSQ 700 Mass Spec-

trometer. The samples were introduced using Atmospheric Pressure Ionization (API) with electrospray. Samples were analyzed in the positive ion mode using a spray voltage of +4500 V, capillary heater temperature of 270°C, sheath gas of 80 psi (N_2), and an auxiliary gas flow (N_2) of 30 ml/min. For full scan analysis, the mass spectrometer was scanned from 150 to 600 amu in 1 s. MS/MS analysis was performed using a collision energy of −30 eV and collision gas pressure of 1.5 mTorr (argon).

In Vitro Studies. In vitro experiments were conducted to aid in the identification/confirmation of metabolite structures when the authentic standards were not available. The rat liver microsomes and cytosolic fraction were prepared by differential centrifugation (van der Hoeven and Coon, 1974). Protein concentrations were determined by the Lowry assay (Lowry et al., 1951).

Incubation of dehydrogenated moxonidine with rat liver microsomes. Briefly, 100 mM sodium phosphate (pH 7.4), 2 mM final concentration of NADPH, and 2 mg/ml final concentration of microsomal protein were added on ice to a final volume of 1 ml. The mixture was preincubated for 3 min at 37°C in a shaking water bath. The reaction was initiated by adding dehydrogenated moxonidine to a final concentration of 100 μM. Control incubations were performed without adding NADPH. The reaction was allowed to proceed in the shaking water bath for 2 h at approximately 37°C, and was terminated by adding 20% TCA (20% v/v of total volume of incubation). The incubation mixtures were then centrifuged to remove participated protein. The supernatant obtained was analyzed directly by LC/MS and LC/MS/MS for metabolite identification.

Incubation of moxonidine with rat GST in the presence of GSH. Incubations were conducted at substrate concentration of 200 μM in a total volume of 1 ml. Sodium phosphate (100 mM, pH 6.8), 10 mM GSH, and 19 U/ml GST were added on ice to a final volume of 1 ml. Control incubations were performed without adding substrate or GST. The reaction was initiated by adding moxonidine and proceeded for 2 h at 25°C. The incubations were terminated by adding 20% TCA. The work-up procedures and LC/MS/MS analysis were the same as above.

Incubation of moxonidine or hydroxymethyl moxonidine with rat liver cytosolic fraction in the presence of GSH. Incubations were performed at 37° for 2 h in 100 mM sodium phosphate (pH 7.4), 1 mM GSH, and cytosolic protein 2 mg/ml in a total volume of 1 ml. Control incubations were performed without adding GSH. After preincubation for 3 min, the reaction was initiated by addition of moxonidine or hydroxymethyl moxonidine to a final concentration of 100 μM. Reactions were terminated by adding 20% TCA. The work-up procedures and LC/MS/MS analysis were the same as above.

Balance Excretion Studies. *In noncannulated animals.* A balance excretion study was conducted in noncannulated male F344 rats dosed with [^{14}C]moxonidine by oral gavage (5 mg/kg or 50 μCi/kg). Urine and fecal samples were collected in steel metabolism cages. Urine samples were collected at 12, 24, 48, 72, 96, and 120 h after dosing, feces were collected at 24-h intervals. Rats were sacrificed by CO_2 asphyxiation at 120 h after dosing, and rat carcasses were retained for determination of residual radioactivity. Cages were rinsed at 120 h with deionized water after collection of urine and feces. All samples were stored at approximately −70°C until analysis.

In bile duct-cannulated animals. A biliary excretion study was conducted in bile duct-cannulated male F344 rats. The individual rat was anesthetized with isoflurane and an abdominal midline incision is made to allow cannulation of the bile duct. A bile duct cannula, attached to a trocar, is passed under the skin and exteriorized through an incision on the back of the neck and secured with a button. The other end of the cannula is inserted into the bile duct and secured with suture. After confirming bile flow, the distal end of the cannula is attached to a tether and swivel, which are connected to a piece of tygon tubing for bile collection. The tether allows free movement of the rat in the cage during the bile collection interval. The animals were administered a single oral dose of 5 mg/kg (or 50 μCi/kg) of [^{14}C]moxonidine within 24 h after the surgery. Nalge metabolism cages were used to collect samples. The bile collection system was equipped with a system that collected samples in polypropylene tubes and kept them frozen during the collection period. Bile was collected at 8-h intervals during the first 24 h; thereafter, 8-h fractions were collected by the bile collection system, then pooled to create samples for each 24-h interval. For the purpose of obtaining a blank matrix for biliary metabolite identification, control bile was collected from a cannulated rat that did not receive an oral dose of [^{14}C]moxonidine. Feces and urine were collected at 24-h intervals. After termination of the live phase, the cages were washed with deionized water and the cage wash was collected. Rats were euthanized at 96 h post dose by CO_2 asphyxiation, and rat carcasses were retained for determination of residual radioactivity.

Sample analysis. The radioactive content of all samples was quantified by liquid scintillation counting using an external standard to measure the efficiency of counting via a channel ratio method. For urine, bile, and cage wash samples, three aliquots were pipetted/weighed into scintillation vials. A 10-ml aliquot of Ultima Gold XR Cocktail (or Beckman Ready scintillant) was added, and the radioactive content of the samples was counted in a liquid scintillation counter. Fecal samples were suspended in an SDS solution (0.5%, w/v), frozen, thawed, and shaken vigorously to give a homogeneous slurry. Three aliquots of each fecal slurry were pipetted into combustion thimbles and weighed. The samples were allowed to dry overnight in a fume hood and were then combusted in a Packard Tricarb Oxidizer 307. The resulting $^{14}CO_2$ was trapped and counted for radioactivity by a Packard Tricarb liquid scintillation analyzer 1600 TR. Rat carcasses were digested by gently boiling in beakers containing 300 ml of ethanol and 50 g of potassium hydroxide until all the tissue was dissolved. The digest solutions were cooled and weighed. Three 200-μl aliquots of the solution were pipetted into scintillation vials and weighed. The samples were mixed with 200 μl of hydrogen peroxide, 200 μl of glacial acetic acid, and 10 ml of Ultima Gold XR Cocktail (or Beckman Ready scintillant), and then were counted by the Packard Tricarb liquid scintillation analyzer.

QWBA Study. QWBA study was conducted in male F344 rats after oral administration of 5 mg/kg of [^{14}C]moxonidine (approximately 56.2 μCi/rat). Rats (one animal per time point) were sacrificed at 1, 2, 4, 6, 12, 24, and 48 h after dosing and processed for whole body autoradiography as described in detail by Ullberg (1977). After euthanasia, using isoflurane and exsanguination via cardiac puncture, each animal was rapidly frozen in hexane cooled with dry ice and stored frozen. To process for whole body autoradiography, the frozen carcasses were embedded in a 2% aqueous gel of carboxymethylcellulose, which when frozen, supported the carcass for sectioning on a cryomicrotome. Sagittal whole body sections (approximately 20-μm thick) were then freeze-dried. Sections were sampled to include the following tissues and organs for qualitative and/or quantitative evaluations: adrenal gland, blood, bone, bone marrow, brain areas (cerebellum, cerebrum, and medulla), brown fat, cecal wall, epididymis, eye, Harderian gland, intestinal wall, kidney, liver, lung, lymph node, muscle, myocardium, pancreas, pituitary gland, preputial gland, prostate gland, salivary gland, seminal vesicles, skin, spleen, spinal cord, stomach wall, testis, thymus, thyroid gland, and white fat. In addition, cecal contents, feces, gastrointestinal contents, and urine were qualitatively evaluated. Autoradiographic images were recorded and quantified using phosphor imaging technology as described in detail by Johnston et al. (1990). Quantitation of tissue concentrations of radioactivity was conducted using radiocarbon commercial standards (American Radiolabeled Chemicals, St. Louis, MO) and a liver homogenate, which was used as an internal standard to correct for section thickness variations. Liver was homogenized with Milli-Q water (1:1, w/w), and [^{14}C]glucose was added to yield a final concentration of 46.19 nCi/g. Sagittal whole body sections, radiocarbon standards, and internal standards were simultaneously exposed for approximately 7 days to phosphor imaging plates (Molecular Dynamics, Sunnyvale, CA). Before exposure, background was erased by exposing the imaging plates to bright visible light using the model 410A Image Eraser (Molecular Dynamics). After exposure, imaging plates were scanned with a helium-neon laser using the model 425E PhosphorImager (Molecular Dynamics). Scanner operations, data display, and analysis were performed using ImageQuant (Molecular Dynamics) and Excel (Microsoft, Redmond, WA) software. Quantitative evaluation was accomplished using volume integrated phosphor imager signals from tissues that were corrected for section thickness variation using the internal standard as described by Chay and Pohland (1994). Single samples were taken from multiple sections for each tissue from each animal. Standard curves associated with individual scans were fit with a least-squares regression line from which tissue concentrations of radiocarbon were interpolated. The reported lower limit of detection (mean level of 0.25 μg-Eq/g and range of 0.0821–0.4021 μg-Eq/g) was based on the mean standard curve concentrations. Phosphor images were also visually evaluated and representative images were reproduced.

TABLE 1

Pharmacokinetic parameters of moxonidine, plasma, and whole blood radioactivity (expressed as moxonidine equivalents) in Fischer 344 rats after i.v. administration of 0.3 mg/kg of [^{14}C]moxonidine

	$AUC_{0\ to\ t}$ [a]	$C_{max\ (observed)}$	$C_{0\ (extrapolated)}$	$T_{max\ (observed)}$	$T_{1/2(\alpha)}$	$T_{1/2(\beta)}$
	ng · h/ml or ng-Eq · h/ml	*ng/ml or ng-Eq/ml*		*h*	*h*	*h*
Plasma moxonidine	93.8	146.0	146.0	0.08	0.9	NC
Plasma radioactivity	396.3	172.6	189.1	0.17	1.4	71.8
Whole blood radioactivity	415.6	216.9	216.9	0.17	1.3	58.9

NC, not calculated.
[a] T = 6 h for plasma moxonidine, and T = 48 h for plasma and whole blood radioactivity.

Results

Pharmacokinetics of Moxonidine. After i.v. administration, the highest observed concentration of moxonidine ($C_{max,\ observed}$) was 146.0 ng/ml at 0.08 h ($T_{max,\ observed}$), and the extrapolated concentration of moxonidine (C_0) was also 146.0 ng/ml. The highest observed concentrations of plasma and whole blood radioactivity were 172.6 and 216.9 ng-Eq/ml, respectively, at 0.17 h, and their corresponding extrapolated C_0 values were 189.1 and 216.9 ng-Eq/ml (Table 1). The extrapolated C_0 values may be slightly underestimated due to the variability in the plasma concentrations (especially the early time points) seen with the staggered sampling design in this study. As shown in Fig. 2, both moxonidine and radioactivity showed a second peak at about 4 h, suggesting that moxonidine undergoes enterohepatic recirculation. The plasma concentrations of moxonidine were BQL after 8 h. However, the total radioactivity in plasma and whole blood remained detectable for up to 48 h and was eliminated at a much slower rate during the second phase. The half-life of moxonidine was calculated to be 0.9 h. The initial half-life ($T_{1/2(\alpha)}$) values for plasma and whole blood radioactivity were calculated to be 1.4 and 1.3 h, respectively, and the terminal elimination half-life ($T_{1/2(\beta)}$) values were 71.8 and 58.9 h, respectively. $AUC_{0\text{-}t}$ values for moxonidine and plasma and whole blood radioactivity were 94.5 ng · h/ml, 396.3 ng-Eq · h/ml, and 415.6 ng-Eq · h/ml, respectively.

After oral administration, the mean maximum plasma concentration of moxonidine (C_{max}) was determined to be 4.0 ng/ml at 0.25 h, which was the first time point measured. Maximum concentrations of plasma and whole blood radioactivity were determined to be 68.4 and 102.6 ng-Eq/ml, respectively, at 0.5 h (Table 2). The mean plasma concentrations of moxonidine were BQL in three of the four samples collected at 4 and 6 h post dose. However, the total radioactivity in plasma and whole blood remained detectable for up to 48 h and was eliminated at a much slower rate during the second phase (Fig. 3). The half-life of moxonidine was calculated to be 1.1 h. The initial half-life ($T_{1/2(\alpha)}$) values for plasma and whole blood radioactivity were calculated to be 1.6 and 1.5 h, respectively, and the terminal elimination half-life ($T_{1/2(\beta)}$) was 50.0 and 32.7 h, respectively. Plasma and whole blood radioactivity $AUC_{0\text{-}t}$ values (345.9 and 376.3 ng-Eq · h/ml, respectively) were comparable, and both were much higher than the $AUC_{0\text{-}t}$ for moxonidine (4.8 ng · h/ml). The significantly greater $AUC_{0\text{-}t}$ values and long terminal half-lives determined for plasma and whole blood radioactivity compared with that determined for moxonidine indicate the presence of metabolite(s) of moxonidine that persist longer than the parent compound. Comparing the $AUC_{0-6\ h}$ of moxonidine after oral (4.8 ng · h/ml) versus i.v. (93.8 ng · h/ml) administration, the oral bioavailability of moxonidine was calculated to be 5.1%. The concentrations and AUC values between plasma and whole blood radioactivity were comparable, suggesting that moxonidine and/or its metabolites likely partitioned into red blood cells.

Metabolite Identification. *Urine.* A reversed phase HPLC method with radiochemical detection was developed to separate urinary metabolites of moxonidine. As shown in Fig. 4, five metabolite peaks (metabolites A, B, C, D, and E) were detected in the rat urine sample collected from 0 to 12 h after oral dose administration. About 55% of the radioactive dose was excreted in urine within 12 h based on balance excretion data. Metabolites D and C, which eluted at approximately 6 and 11 min, respectively, were the two major metabolites; they represented 23.0 and 26.2% of the urinary radioactivity, respectively. Other minor metabolites, A, B, and E, accounted for about 1.90, 7.6, and 6.7% of the urinary radioactivity, respectively. Other small peaks accounted for approximately 7% of the urinary radioactivity. About 10.5% of the radioactivity was accounted for as unchanged moxonidine, indicating that moxonidine was extensively metabolized in rats. The recovery of radioactivity from HPLC column was approximately 83%. The structural identification of moxonidine metabolites was performed by positive-ion LC/MS and LC/MS/MS. Several metabolites were positively identified based on retention time and spectral comparison to the authentic standards. In the case that structural identification was unable to be confirmed due to lack of authentic standard, in vitro studies have been used to gain additional information to support the structural assignments.

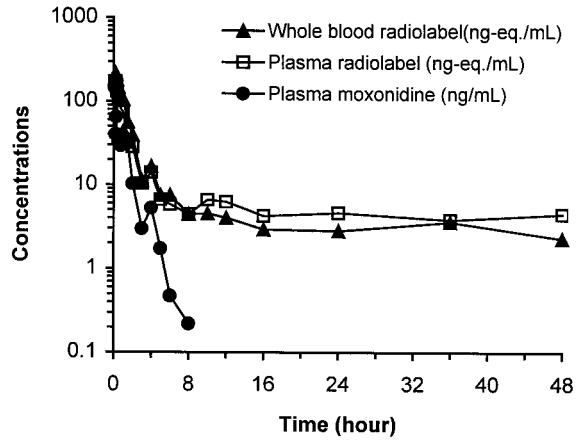

FIG. 2. *Concentrations of moxonidine and radioequivalents of moxonidine in plasma and whole blood after i.v. administration of 0.3 mg/kg of [^{14}C]moxonidine to F344 rats.*

The positive product ion mass spectrum of the moxonidine standard at m/z 242 is shown in Fig. 5, along with a proposed fragmentation pattern. The product ion mass spectrum exhibits prominent fragment ions at *m*/*z* 206, 199, 149, 137, 123, 56, and 44. The base fragment ion at *m*/*z* 199 represents the loss of the 44 amu from the imidazoline ring. This type of fragmentation pattern was confirmed by a deuterium exchange experiment, i.e., *m*/*z* 200 and 45 were detected after two protons located on nitrogen atoms in the imidazoline ring were exchanged by deuterium. The fragment ion at *m*/*z* 206 results from the loss of chlorine. Prepared samples were initially analyzed in full scan positive ion mode (50–600 amu). In addition to the detection of

TABLE 2

Pharmacokinetic parameters of moxonidine, plasma, and whole blood radioactivity (expressed as moxonidine equivalents) in Fischer 344 rats after oral administration of 0.3 mg/kg of [^{14}C]moxonidine

	$AUC_{0\ to\ t}$[a]	C_{max}	T_{max}	$T_{1/2(\alpha)}$	$T_{1/2(\beta)}$
	ng · h/ml or ng-Eq; h/ml)	*ng/ml or ng-Eq/ml*	*h*	*h*	*h*
Plasma moxonidine	4.8	4.0	0.25	1.1	NC
Plasma radioactivity	345.9	68.4	0.5	1.6	50.0
Whole blood radioactivity	376.3	102.6	0.5	1.5	32.7

NC, not calculated.
[a] T = 6 h for plasma moxonidine, and T = 48 h for plasma and whole blood radioactivity.

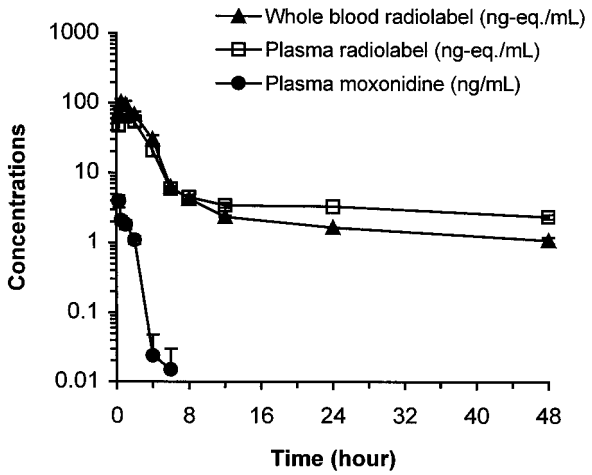

FIG. 3. *Mean (± S.E.) concentrations of moxonidine and radioequivalents of moxonidine in plasma and whole blood after oral administration of 0.3 mg/kg of [^{14}C]moxonidine to F344 rats (n = 4 per time point).*

parent compound (*m*/*z* 242), metabolites (A-E) were detected at *m*/*z* 240, 256, 258, 272, and 434, respectively (Table 3). The characterization of each urinary metabolite is described as follows.

Dehydrogenated moxonidine (metabolite A). This metabolite yields a molecular ion of *m*/*z* 240, which is 2 amu less than parent moxonidine, indicating the loss of two hydrogen atoms from the imidazoline ring. In addition, the dehydrogenated moxonidine gives fragment ions at *m*/*z* 121, 135, 147, and 204, which are 2 amu less than the corresponding fragment ions observed for the moxonidine standard (Table 3). The product ion mass spectrum of metabolite A at *m*/*z* 240 is identical with that of an authentic standard of dehydrogenated moxonidine. The HPLC retention time of this metabolite peak also matched that of the authentic standard.

Hydroxymethyl dehydrogenated moxonidine (metabolite B). This metabolite has a protonated molecular ion of *m*/*z* 256, which is 14 amu higher than parent moxonidine, or 16 amu higher than dehydrogenated moxonidine at *m*/*z* 240. Two possible structures, hydroxymethyl dehydrogenated moxonidine (where the hydroxy group is located on the methyl group of the pyrimidine ring) or a ketone metabolite (ketone group located on the imidazoline ring), were initially proposed for this metabolite, because the addition of 16 amu to the compound at *m*/*z* 240 could indicate hydroxylation, or addition of 14 amu to moxonidine at *m*/*z* 242 could be the formation of a ketone metabolite of moxonidine. LC/MS/MS analysis of an authentic standard of the ketone metabolite excluded the possibility of the ketone metabolite since it produced a product ion mass spectrum different from that of metabolite B. To further support the identification of this metabolite, dehydrogenated moxonidine (metabolite A) was incubated with rat liver microsomes. A hydroxylated metabolite (*m*/*z* 256) that is 16 amu higher than dehydrogenated moxonidine was generated, and the product ion mass spectrum of this in vitro metabolite (*m*/*z* 256) is identical to the metabolite B found in rat plasma, urine, and bile samples, strongly suggesting that metabolite B is hydroxymethyl-dehydrogenated moxonidine.

Hydroxymethyl moxonidine (metabolite C). This metabolite yielded a molecular ion of *m*/*z* 258, which is 16 amu higher than parent moxonidine. The product ion mass spectrum of this major metabolite (shown in Fig. 6) is identical with that of an authentic standard of the hydroxymethyl moxonidine (where the hydroxy group is located on the methyl group of the pyrimidine ring), with prominent fragment ions at *m*/*z* 228, 222, 215, 192, 151, and 44. In addition, HPLC retention time of this metabolite matched that of the authentic standard.

Carboxylic acid metabolite (metabolite D). This metabolite has a protonated molecular ion of *m*/*z* 272 that is 30 amu higher than parent moxonidine (*m*/*z* 242). The product ion spectrum of metabolite D (shown in Fig. 6) and prominent fragment ions of this metabolite at *m*/*z* 192, 177, 165, and 150 are the same as that obtained from the authentic standard of the carboxylic acid metabolite. The HPLC retention time of this major metabolite also matched that of the authentic standard.

Putative glucuronide conjugate of hydroxymethyl moxonidine (metabolite E). This metabolite yielded a molecular ion of *m*/*z* 434. The product ion mass spectrum does show fragment ions at *m*/*z* 258, 228, and 222 (Table 3), which were present in the spectrum of the hydroxymethyl moxonidine (metabolite C, *m*/*z* 258). The loss of 176 amu from the molecular ion of *m*/*z* 434 to 258 indicates that this metabolite is most likely a glucuronide conjugate. The compound is tentatively identified as a glucuronide conjugate of hydroxymethyl moxonidine.

Plasma. Plasma samples from individual time points (1, 2, and 4 h post dose) were pooled, extracted, and analyzed by LC/MS and LC/MS/MS for metabolite identification. In addition to the parent compound, four metabolites (A, B, C, and D) were identified in the plasma extracts (Table 3). Dehydrogenated moxonidine, hydroxymethyl moxonidine, and the carboxylic acid metabolite of moxonidine were definitively identified by comparison of their mass spectra to the mass spectra of authentic standards. Hydroxymethyl dehydrogenated moxonidine (metabolite B) was also identified and it produced the product ion mass spectrum identical to that obtained from urine sample. The levels of moxonidine metabolites appear to be the highest in the plasma sample collected at 1 h post dose.

Bile. Bile samples were analyzed by HPLC, LC/MS, and LC/MS/MS. At least fifteen metabolites were identified or tentatively identified (Table 3). Besides parent moxonidine and metabolites that had been identified in urine samples (metabolites A-E), additional metabolites were detected at *m*/*z* 216, 327, 343, 361, 384, 400, 418, 513, 529, and 547. The characterization of additional biliary metabolites is described as follows.

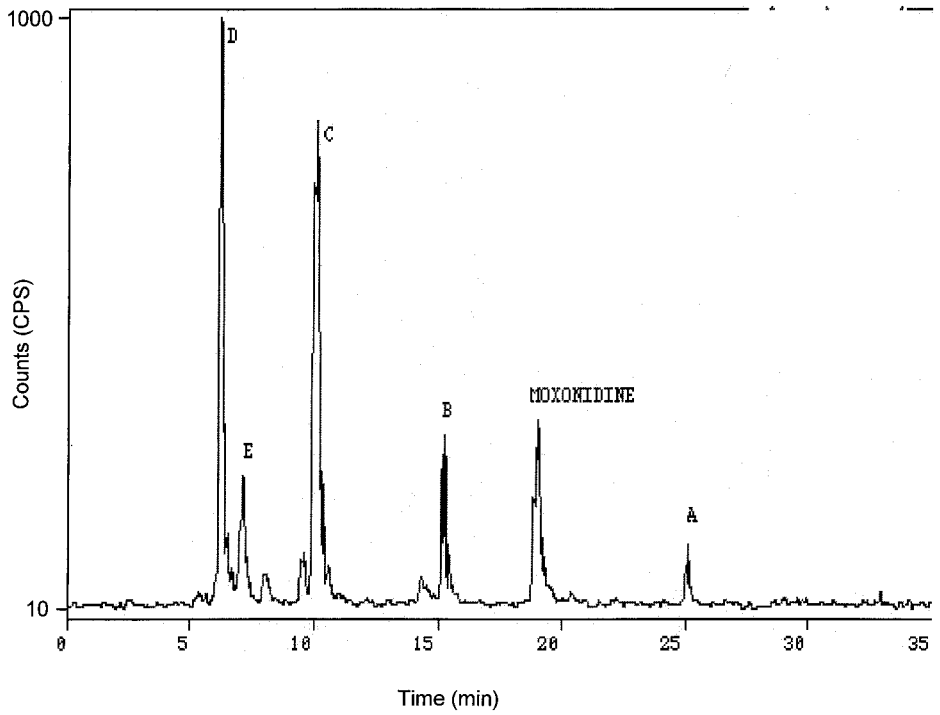

FIG. 4. *HPLC radiochromatogram of rat urine collected from 0 to 12 h after oral administration of 5 mg/kg of [^{14}C]moxonidine.*

A: Dehydrogenated moxonidine; B: Hydroxymethyl dehydrogenated moxonidine; C: Hydroxymethyl moxonidine; D: Carboxylic acid metabolite; E: Glucuronide conjugate of hydroxymethyl moxonidine.

Guanidine metabolite (metabolite F). This metabolite yielded a molecular ion of *m*/*z* 216. The product ion mass spectrum of this metabolite exhibits prominent fragment ions at *m*/*z* 56, 143, 159, 184, and 199, which are identical with that of the guanidine metabolite authentic standard. The HPLC retention time of metabolite F also matched that of the authentic standard, confirming that metabolite F is the guanidine metabolite of moxonidine.

Putative GSH conjugate of moxonidine (metabolite G). The product ion mass spectrum of metabolite G is shown in Fig. 7. This metabolite has a molecular ion of *m*/*z* 547, which is 305 amu higher than moxonidine. The loss of 129 amu (glutamyl moiety) from *m*/*z* 547 to produce a fragment at *m*/*z* 418 suggests that this metabolite is likely a GSH conjugate of moxonidine, and the glutathione is probably located on the imidazoline ring (structure shown in Fig. 8). The fragment ions at *m*/*z* 418, 361, 274, and 240 (base ion) are likely to be the products formed by cleavage of the peptide chain of the glutathione moiety. The major ions at *m*/*z* 240 and 274 were also found in the product ion spectra of metabolite J (cysteinylglycine conjugate) and metabolite M (cysteine conjugate) as described below. A definitive identification of this metabolite needs to be verified by the analysis of an authentic standard.

GSH conjugate of moxonidine minus chlorine (metabolite H). The product ion mass spectrum of metabolite H (*m*/*z* 513) is shown Fig. 7. The loss of 129 amu (glutamyl moiety) from molecular ion *m*/*z* 513 to produce a fragment ion at *m*/*z* 384 suggests that this metabolite is a GSH conjugate. A possible structure for the metabolite at *m*/*z* 513 is a GSH conjugate minus chlorine where the chlorine moiety on the pyrimidine ring of moxonidine was replaced by the glutathione moiety. This assignment is based on the characteristics of the product ion mass spectrum and the absence of the chlorine isotope observed with this metabolite. The fragment ions at *m*/*z* 384, 327 (weak), 281, and 240 (base ion) are likely to be the products formed by cleavage of the peptide chain of the GSH moiety. In fact, two other bile metabolites with molecular ion at *m*/*z* 384 and 327 were identified as cysteinylglycine conjugate and cysteine conjugate (metabolites K and N), respectively, and both produce fragment ions at *m*/*z* 281 and 240 (base ion). The base peak at *m*/*z* 240 is likely a thiol metabolite (the chlorine moiety on the pyrimidine ring of moxonidine was replaced by the thiol) that results from additional degradation of cysteine conjugate. Additional evidence to support the structural assignment of a GSH conjugate minus chlorine was provided by two additional in vitro studies: 1) incubation of moxonidine with rat GST in the presence of GSH, and 2) incubations of moxonidine with rat liver cytosolic fraction in the presence of GSH. The same metabolite (molecular ion at *m*/*z* 513) was generated from both incubations and the product ion spectrum of this in vitro metabolite was identical with that of metabolite H detected in rat bile samples. Additionally, this metabolite (*m*/*z* 513) was generated as a major metabolite in rat liver slice incubations with moxonidine (M.M.H., unpublished data).

Hydroxymethyl GSH conjugate minus chlorine (metabolite I). This metabolite has a protonated molecular ion of *m*/*z* 529. The loss of 129 amu from *m*/*z* 529 to produce a fragment ion at *m*/*z* 400 suggests that this is also a GSH conjugate. This metabolite at *m*/*z* 529 is 16 amu higher than that of metabolite H (*m*/*z* 513), which was identified as a GSH conjugate minus chlorine. The fragment ions at *m*/*z* 400, 297, and 256 (base ion) are 16 amu higher that the corresponding ions present in the spectrum of metabolite H (*m*/*z* 384, 281, and 240, respectively), and they are likely to be the products formed by cleavage of the peptide chain of the GSH moiety. Therefore, this metabolite was identified as the hydroxymethyl GSH conjugate minus chlorine, a hydroxylated species of metabolite H. The structural assignment of this metabolite was also supported by the in vitro approach. Incubation of hydroxymethyl moxonidine (metabolite C) with rat liver cytosolic fraction in the presence of GSH generated a metabolite with a molecular ion at *m*/*z* 529. This in vitro produced metabolite produced an identical product ion mass spectrum to that

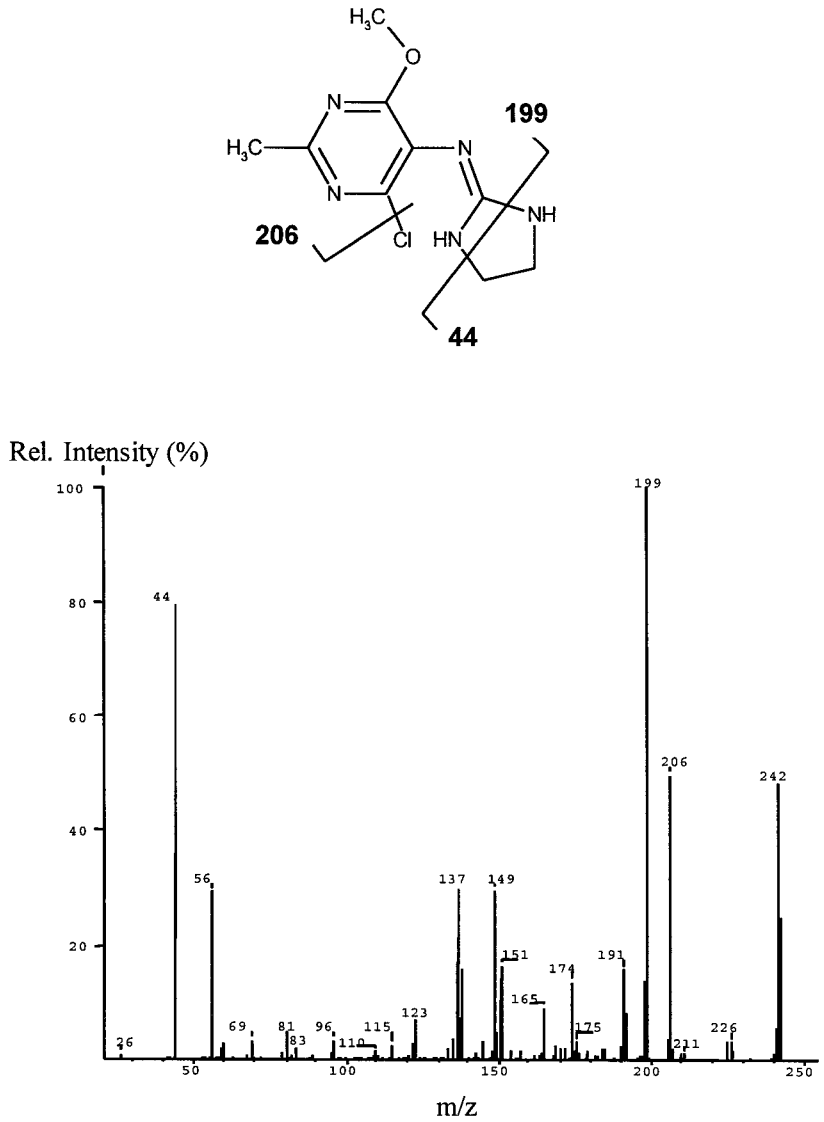

FIG. 5. *Product ion mass spectrum of m/z 242 for moxonidine standard and chemical structure of moxonidine with a proposed fragmentation pattern.*

obtained from metabolite I (*m*/*z* 529) in rat bile, confirming that metabolite I is hydroxymethyl GSH conjugate minus chlorine.

Putative cysteinylglycine conjugate of moxonidine (metabolite J). This metabolite yielded a molecular ion of *m*/*z* 418, which is 176 amu higher than moxonidine, suggesting that it is probably a glucuronide conjugate. However, the base ion observed in the product ion mass spectrum is *m*/*z* 240 which is 2 amu less than moxonidine. The major fragment ions, such as *m*/*z* 204, 240 (base ion), and 274 were also observed in the product ion mass spectrum of metabolite G. The proposed structure for this metabolite is a cysteinylglycine conjugate of moxondine, a product formed by removal of the glutamyl moiety (129 amu) from GSH conjugate (metabolite G, *m*/*z* 547). The definitive identification of this metabolite would need to be verified by the analysis of an authentic standard.

Putative cysteinylglycine conjugate minus chlorine (metabolite K). This metabolite has a protonated molecular ion of *m*/*z* 384, which is 129 amu less than metabolite H (*m*/*z* 513). The major fragment ions obtained for this metabolite, such as *m*/*z* 281, 240 (base ion), 223, and 206 were also observed in the spectrum of metabolite H (Table 3). In addition, this metabolite is 34 amu less than metabolite J (*m*/*z* 418) and no chlorine isotope was present. A tentative assignment for this compound is the cysteinylglycine conjugate minus chlorine, a product formed by removal of the glutamyl moiety from the GSH conjugate minus chlorine (metabolite H, *m*/*z* 513).

Putative hydroxymethyl cysteinylglycine conjugate minus chlorine (metabolite L). This metabolite yielded a molecular ion of *m*/*z* 400. This compound is 16 amu higher than metabolite K (*m*/*z* 384). In fact, many of the product ions detected in metabolite L (e.g., *m*/*z* 256, 297) are 16 amu higher than the product ions detected in metabolite K (e.g., *m*/*z* 240, 281). This compound is most likely the hydroxylated species of metabolite K (*m*/*z* 384), that is a hydroxymethyl cysteinylglycine conjugate minus chlorine. In addition, metabolite L is 129 amu less than metabolite I (*m*/*z* 529), and the major fragment ions obtained for this metabolite, such as *m*/*z* 297, 256 (base ion), and 238, were also observed in the spectrum of metabolite I (*m*/*z* 529), which further confirms that this metabolite is the hydroxymethyl cysteinylglycine conjugate formed from hydrolysis of glutamyl moiety from the hydroxymethyl GSH conjugate minus chlorine (metabolite I).

Putative cysteine conjugate (metabolite M). This metabolite has a protonated molecular ion of *m*/*z* 361. The major fragment ions in product ion spectrum of metabolite M, such as *m*/*z* 274, 240 (base ion), and 204, were also observed in the spectrum of metabolite G

TABLE 3

Moxonidine metabolites identified in rat urine, plasma, and bile after oral administration of [^{14}C]moxonidine

Metabolite	$[M+H]^+$	Characteristic Product Ions	Identification	Urine	Plasma	Bile
		m/z				
	242	44, 123, 137, 149, 199, 206	Parent	√	√	√
A[a]	240	56, 121, 135, 147, 159, 184, 204, 224	Dehydrogenated moxonidine	√	√	√
B[b]	256	72, 94, 121, 133, 149, 161, 170, 190, 202, 220, 226	Hydroxymethyl dehydrogenated moxonidine	√	√	√
C[a]	258	44, 135, 137, 151, 192, 215, 222, 228	Hydroxymethyl moxonidine	√	√	√
D[a]	272	150, 151, 165, 177, 192	Carboxylic acid metabolite	√	√	√
E	434	222, 228, 258	Putative glucuronide conjugate of hydroxymethyl moxonidine	√		√
F[a]	216	56, 143, 159, 184, 199	Guanidine metabolite			√
G	547	204, 240, 274, 418	Putative GSH conjugate			√
H[b]	513	145, 223, 240, 281, 384	GSH conjugate minus chlorine			√
I[b]	529	86, 145, 238, 256, 297, 400	Hydroxymethyl GSH conjugate minus chlorine			√
J	418	204, 240, 274,	Putative cysteinylglycine conjugate			√
K	384	206, 223, 240, 281,	Putative cysteinylglycine conjugate minus chlorine			√
L	400	86, 205, 238, 256, 297	Putative hydroxymethyl cysteinylglycine conjugate minus chlorine			√
M	361	204, 240, 274	Putative cysteine conjugate			√
N[a]	327	205, 223, 240, 281	Cysteine conjugate minus chlorine			√
O	343	204, 238, 256	Putative hydroxymethyl cysteine conjugate minus chlorine			√

[a] Identification was confirmed by corresponding authentic standard.
[b] Identification was supported by the results of in vitro studies.

(*m/z* 547) and metabolite J (*m/z* 418). This compound is likely the cysteine conjugate formed by additional removal of the glycyl moiety from the cysteinylglycine conjugate (metabolite J).

Cysteine conjugate minus chlorine (metabolite N). This metabolite has a protonated molecular ion of *m/z* 327. The product ion mass spectrum of metabolite N is identical to that of an authentic standard. The major fragment ions obtained for this metabolite, such as *m/z* 281, 240 (base ion), and 223, were also observed in the spectrum of metabolite H (*m/z* 513) and K (*m/z* 384). This metabolite is likely formed by additional removal of the glycyl moiety from the cysteinylglycine conjugate minus chlorine (metabolite K, *m/z* 384).

Putative hydroxymethyl cysteine conjugate minus chlorine (metabolite O). This metabolite yielded a molecular ion of *m/z* 343. The major fragment ions in product ion spectrum obtained for this metabolite, such as *m/z* 204, 238, and 256, were also observed in the spectrum of metabolite L (*m/z* 400). This compound is probably the hydroxymethyl cysteine conjugate minus chlorine formed by additional removal of the glycine moiety from the hydroxymethyl cysteinylglycine conjugate minus chlorine (metabolite L).

Radiocarbon Excretion. Balance excretion studies were conducted in noncannulated and bile duct-cannulated male F344 rats administered a single oral dose of 5 mg/kg of [^{14}C]moxonidine (free base). Residual radioactivity of urine, feces, bile, cage washes, and carcasses were determined by liquid scintillation counting. In noncannulated rats (as shown in Table 4), the mean (±S.E.) total recovery of radioactivity within 120 h was 100.25 ± 1.19%, with 59.46 ± 4.29% in the urine, 38.40 ± 2.65% in the feces, 2.02 ± 0.68% in the cage wash, and 0.37 ± 0.04% remaining in the carcass. The excretion of the radioactivity in both urine and feces was virtually complete within 24 h after oral administration. The elimination profiles of radioactivity indicate that urinary excretion is the primary route of elimination for the radioactivity. The radioactivity administered was also excreted partially in the feces but to a lesser extent.

In bile duct-cannulated rats (as shown in Table 5), the mean (±S.E.) total recovery of radioactivity within 96 h was 78.47 ± 2.02%, with 39.74 ± 0.10% in the urine, 32.60 ± 0.02% in the bile, 2.33 ± 0.16% in the feces, 2.34 ± 0.52% in the cage wash, and 1.46 ± 0.30% remaining in the carcass. Urinary excretion was found to be the primary route of elimination in cannulated rats, but biliary excretion also contributed to the eliminate of radioactivity in rats as 32.6% of total radioactivity was excreted in the bile. The elimination profiles of radioactivity determined from both noncannulated and bile duct-cannulated rats suggest that moxonidine is well absorbed, and that the radiocarbon is mainly eliminated in urine, but also excreted into bile.

Quantitative Whole Body Autoradiography. Table 6 shows radiocarbon tissue concentrations determined by quantitative whole body autoradiography. At 1 h post dose, radioactivity associated with [^{14}C]moxonidine was rapidly absorbed and distributed to all major tissues (Fig. 9). The highest concentrations of radiocarbon were determined in the kidney and liver with both tissues displaying differential distributions of 5.41 to 18.14 and 4.57 to 20.48 μg-Eq/g, respectively. Many tissues contained moderate concentrations of radioactivity at this time point. These tissues included blood, Harderian gland, intestinal wall, lung, pancreas, prostate gland, salivary gland, and stomach wall with concentrations ranging from 1.04 to 2.81 μg-Eq/g. All other tissues contained low or background levels of radioactivity at 1 h post dose. Peak tissue concentrations of radiocarbon occurred at 2 h post dose in most tissues with the exception of blood, liver, lung, pancreas, prostate gland, and stomach wall, which had a T_{max} of 1 h post dose. At 2 and 4 h post dose, high levels of radioactivity continued to be found in the kidney and liver with high concentrations ranging from 6.31 to 32.44 μg-Eq/g. Many tissues contained moderate concentrations of radioactivity at these time points. At 2 h post dose, adrenal, blood, Harderian gland, intestinal wall, pancreas, salivary gland, and stomach wall had concentrations ranging from 1.0 to 1.76 μg-Eq/g. By 4 h post dose, most tissue concentrations were low with the radiocarbon concentrations ranging from 0.25 to 0.66 μg-Eq/g. At 6 and 12 h post dose, concentrations of radiocarbon in all tissues had declined to low or undetectable concentrations. The highest concentrations of radiocarbon continued to be found in the kidney and liver and these concentrations declined from 6.53 to 0.85 and 4.29 to 1.76 μg-Eq/g, respectively, over the 6- and 12-h time points. Low concentrations of radiocarbon were detected at

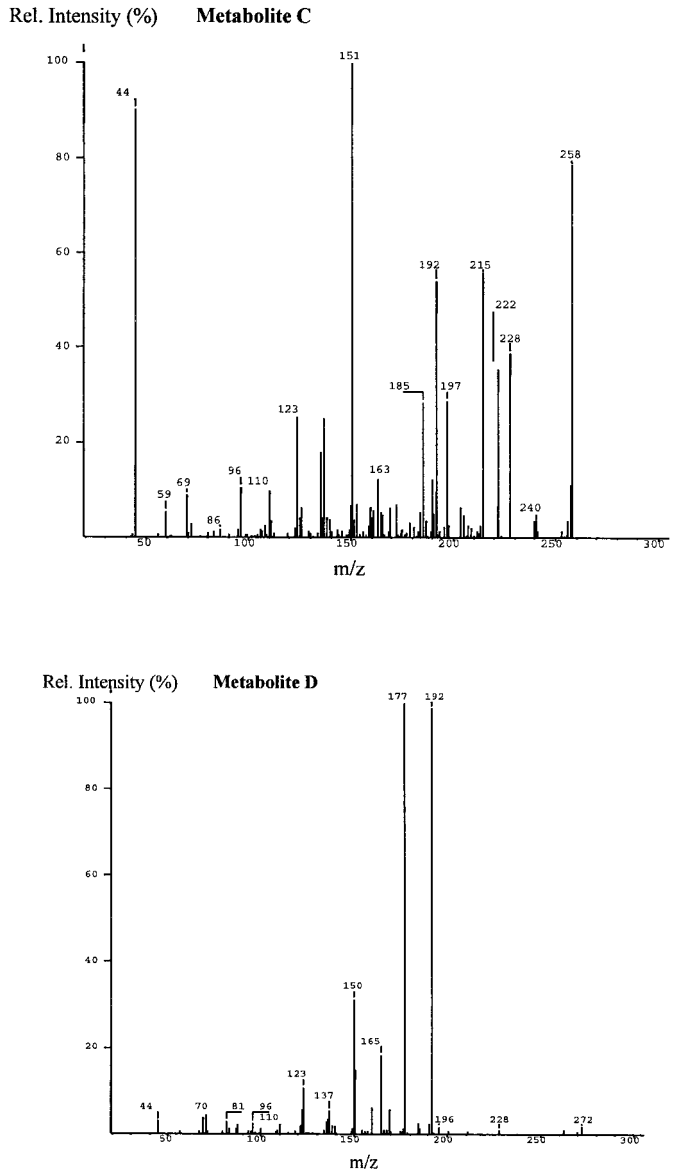

FIG. 6. *Product ion mass spectra of major metabolites C and D (at m/z 258 and 272, respectively) present in a rat urine sample collected at 0 to 12 h post dose.*

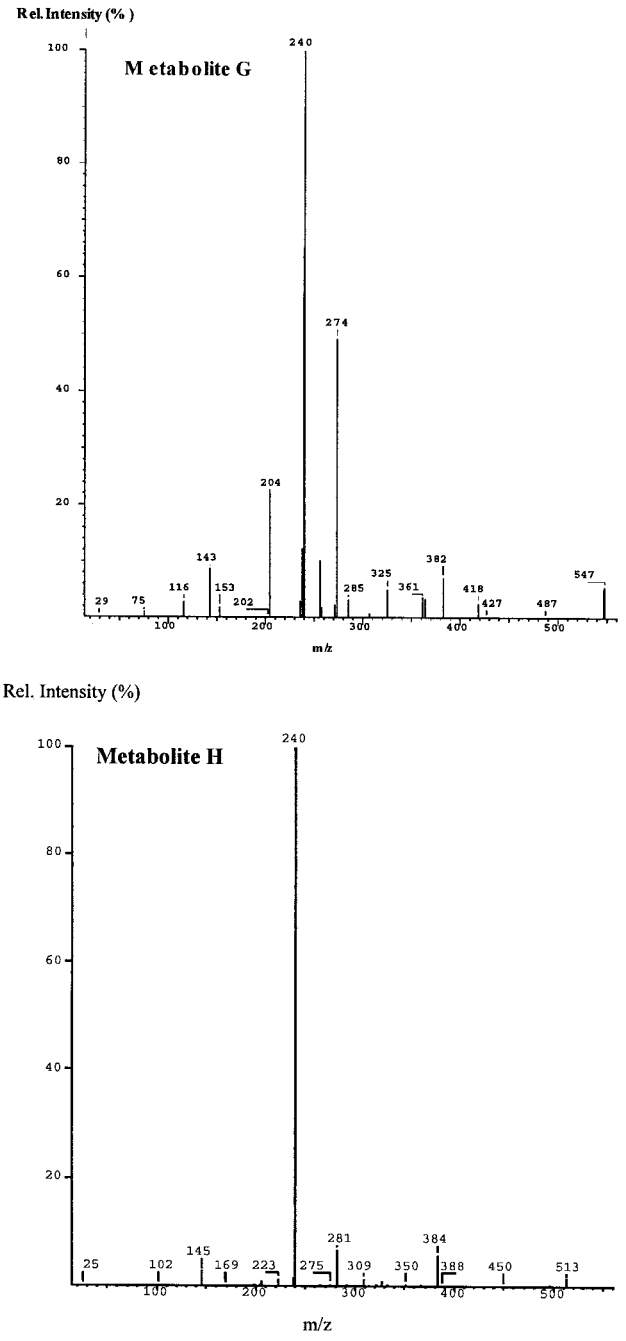

FIG. 7. *Product ion mass spectra of metabolites G and H (at m/z 547 and 513, respectively) present in a rat bile sample collected at 0 to 8 h post dose.*

6 h in eye, Harderian gland, pancreas, salivary gland, and stomach wall ranging from 0.29 to 0.80 μg-Eq/g, but these values were nondetectable at 12 h post dose. At 24 and 48 h post dose, radiocarbon associated with most tissues had decreased to low or background levels, except for the liver, where the concentration was 0.42 μg-Eq/g at 48 h post dose.

Pharmacokinetic parameters were calculated for different tissues in the male Fischer 344 rats (Table 7). The estimated half-lives for radiocarbon ranged from approximately 1.46 h in the lung to 20.15 h in the liver. Due to the rapid elimination from the tissues, the half-lives could not be calculated for most of the tissues. AUC values were the greatest in the kidney and the liver with $AUC_{0\text{-}\infty}$ values of approximately 129.34 and 103.53 μg-Eq · h/g, respectively.

Discussion

Three lines of evidence have been obtained that suggest that moxonidine is extensively metabolized in rats after oral administration. The first is that comparison of plasma concentrations, as well as AUC values, between plasma radioactivity and parent moxonidine indicated large amount of circulating metabolites in the plasma. The second is that the bioavailability of moxonidine (5.1%), as determined from pharmacokinetic studies after i.v. and oral doses of moxonidine, was quite low. This is in contrast to what has been observed in humans in which the absolute bioavailability is quite high (approximately 88%, Schaefer et al., 1998). The low bioavailability in rats can be caused by poor absorption or by extensive first-pass metabolism. Because moxonidine is well absorbed based on the balance excretion data, first-pass metabolism accounts for the low bioavailability of moxonidine in rats. The third was that a number of moxonidine metabolites were identified in rat plasma, urine, and bile samples collected after oral administration of moxonidine.

A proposed metabolic scheme for the metabolism of moxonidine in rats is shown in Fig. 8. The metabolic attack can occur at both

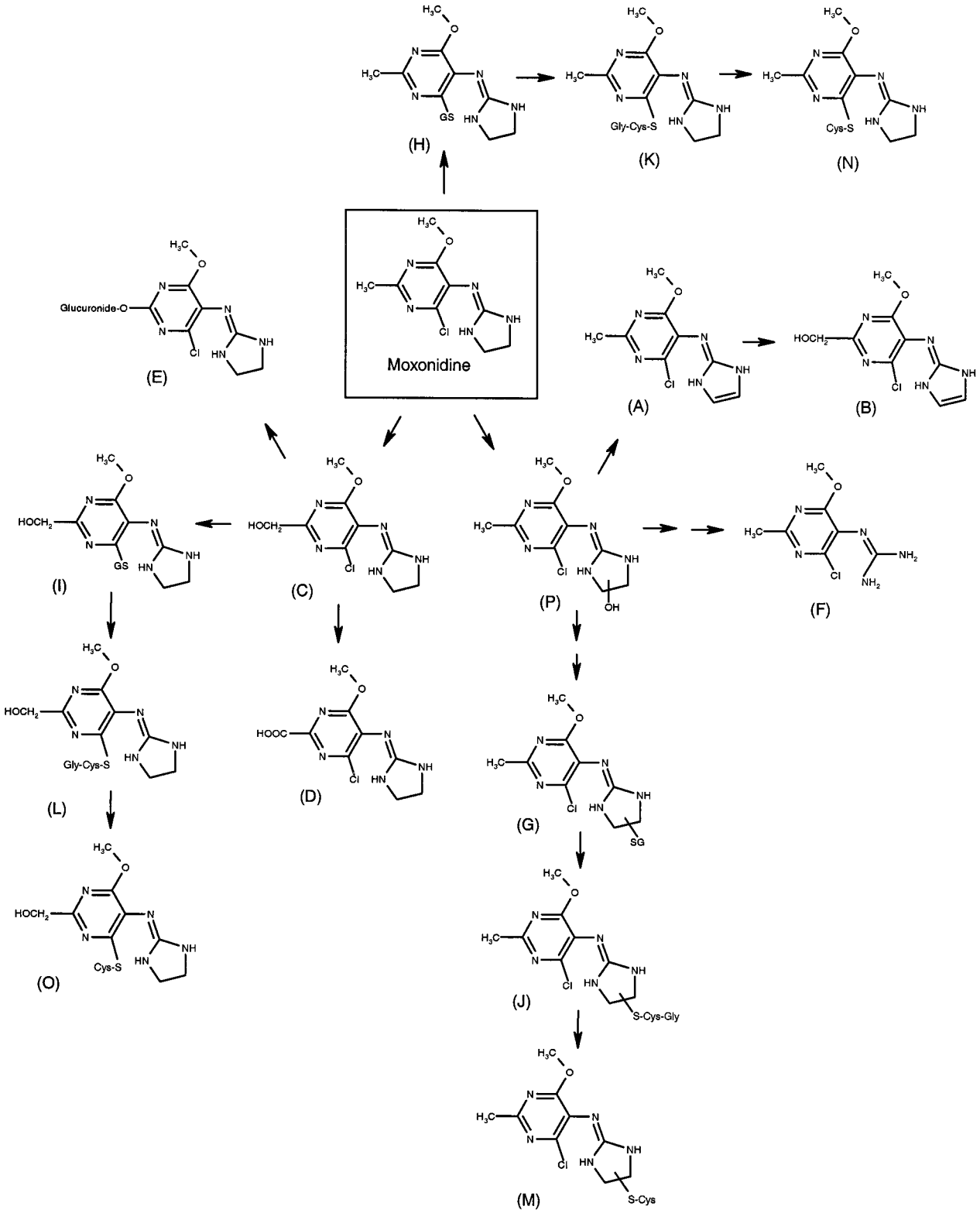

FIG. 8. *Proposed metabolic scheme of moxonidine in rats.*

the pyrimidine ring (on methyl group) and the imidazoline ring, resulting in the formation of variety of phase I and phase II metabolites. Initially, moxonidine undergoes oxidation (phase I metabolism) to form either hydroxymethyl moxonidine (metabolite C, with hydroxy group located on methyl group) or a hydroxy moxonidine intermediate (metabolite P, with hydroxy group located on the imidazoline ring). Additional oxidation of hydroxymethyl moxonidine (metabolite C) leads to the formation of the carboxylic acid metabolite (D). The hydroxy moxonidine (metabolite P) either loses water to form dehydrogenated moxonidine (metabolite A), which is then oxidized to hydroxymethyl dehydrogenated moxonidine (metabolite B), or decomposes to a ring-

TABLE 4

Mean (±S.E.) cumulative elimination of radioactivity from male Fischer 344 rats after a single oral dose of 5 mg/kg of [^{14}C]moxonidine

h	*N*	Percentage of Dose (±S.E.M)				
		Urine	Feces	Carcass	Cage Wash	Total
12	3	55.00 ± 6.59				55.00 ± 6.59
24	3	58.22 ± 4.79	36.37 ± 1.96			94.59 ± 2.85
48	3	58.89 ± 4.46	37.93 ± 2.67			96.82 ± 1.79
72	3	59.08 ± 4.48	38.20 ± 2.64			97.28 ± 1.84
96	3	59.35 ± 4.32	38.32 ± 2.65			97.66 ± 1.68
120	3	59.46 ± 4.29	38.40 ± 2.65	0.37 ± 0.04	2.02 ± 0.68	100.25 ± 1.19

TABLE 5

Mean (±S.E.) cumulative elimination of radioactivity from bile duct-cannulated male Fischer 344 rats after a single oral dose of 5 mg/kg of [^{14}C]moxonidine

h	*N*	Percentage of Dose (±S.E.M.)					
		Urine	Feces	Bile	Carcass	Cage Wash	Total
8	4			30.75 ± 4.34			30.75 ± 4.34
16	4			31.95 ± 0.58			31.95 ± 0.58
24	4	34.30 ± 1.60	0.51 ± 0.22	32.20 ± 0.08			67.02 ± 4.48
48	4	37.83 ± 0.96	1.26 ± 0.17	32.50 ± 0.10			71.59 ± 3.58
72	4	39.18 ± 0.47	1.94 ± 0.35	32.58 ± 0.03			73.70 ± 2.81
96	4	39.74 ± 0.10	2.33 ± 0.16	32.60 ± 0.02	1.46 ± 0.30	2.34 ± 0.52	78.47 ± 2.02

TABLE 6

Mean tissue concentrations of radiocarbon (μg-Eq/g) in male Fischer 344 rats after a single oral dose of 5-mg/kg of [^{14}C]moxonidine

Tissue	Concentrations of Radiocarbon						
	1 h	2 h	4 h	6 h	12 h	24 h	48 h
				μg-Eq/g			
Adrenal	#	1.17	0.44	ND	ND	ND	ND
Blood	1.19	1.07	0.25	ND	ND	ND	ND
Bone Marrow	0.56	0.66	ND	ND	ND	ND	ND
Brown Fat	0.41	0.57	ND	ND	ND	ND	ND
Epididymis	0.30	0.50	0.31	#	ND	ND	ND
Eye	0.40	0.74	ND	0.59	ND	ND	ND
Harderian Gland	1.25	1.76	1.02	0.80	ND	ND	ND
Intestinal Wall	1.09	1.34	0.55	#	#	ND	ND
Kidney-High	18.14	32.44	17.45	6.53	0.85	0.33	ND
Kidney-Low	5.41	3.83	1.29	0.35	ND	ND	ND
Liver-High	20.48	16.44	6.31	4.29	1.76	0.44	0.42
Liver-Low	4.57	5.61	1.91	0.86	0.36	ND	ND
Lung	1.09	0.93	0.28	ND	ND	ND	ND
Lymph Nodes	0.59	0.7	ND	NS	NS	NS	NS
Muscle	0.41	0.56	ND	ND	ND	ND	ND
Myocardium	0.67	0.68	ND	ND	ND	ND	ND
Pancreas	1.60	1.00	0.41	0.29	ND	ND	ND
Pituitary Gland	0.89	0.92	ND	ND	ND	ND	ND
Preputial Gland	0.69	0.81	#	#	ND	ND	ND
Prostate Gland	1.30	#	#	#	#	ND	ND
Salivary Gland	1.04	1.41	0.66	0.34	ND	ND	ND
Seminal Vesicles	ND	0.52	0.49	ND	ND	ND	ND
Skin	0.53	0.67	ND	ND	ND	ND	ND
Spleen	#	0.7	#	ND	ND	ND	ND
Stomach Wall	2.81	1.70	0.43	0.45	ND	ND	ND
Testes	0.19	0.41	ND	ND	ND	ND	ND
Thymus	0.50	0.68	ND	ND	ND	ND	ND
Thyroid Gland	0.89	0.98	0.45	ND	ND	ND	ND

ND, Not Detectable (below limit of detection).
#, Tissue was not sampled due to quality of section.
NS, No Sample.

opened intermediate, generating the guanidine metabolite (F). Hydroxy moxonidine (metabolite P) was not detected in vivo, probably because it was quickly converted to secondary metabolites (i.e., metabolites A, F, or G) once it was generated. This hydroxy metabolite was positively identified in in vitro incubations with rat, monkey, dog, and human liver microsomes (M.M.H., unpublished data). Most of the phase I metabolites were identified in plasma, urine, and bile samples. The HPLC radiochromatographic profiles of urine revealed that hydroxymethyl moxonidine (metabolite C) and the carboxylic acid metabolite (metabolite D) were the major metabolites, suggesting that oxidation of the methyl group represents the major oxidative pathway. Hydroxymethyl moxonidine was also generated in in vitro incubations with rat liver microsomes or rat liver slices, and it was also formed in vivo in mice, dogs, and humans (M.M.H., unpublished data). However, the additional oxidation product, the carboxylic acid metabolite,

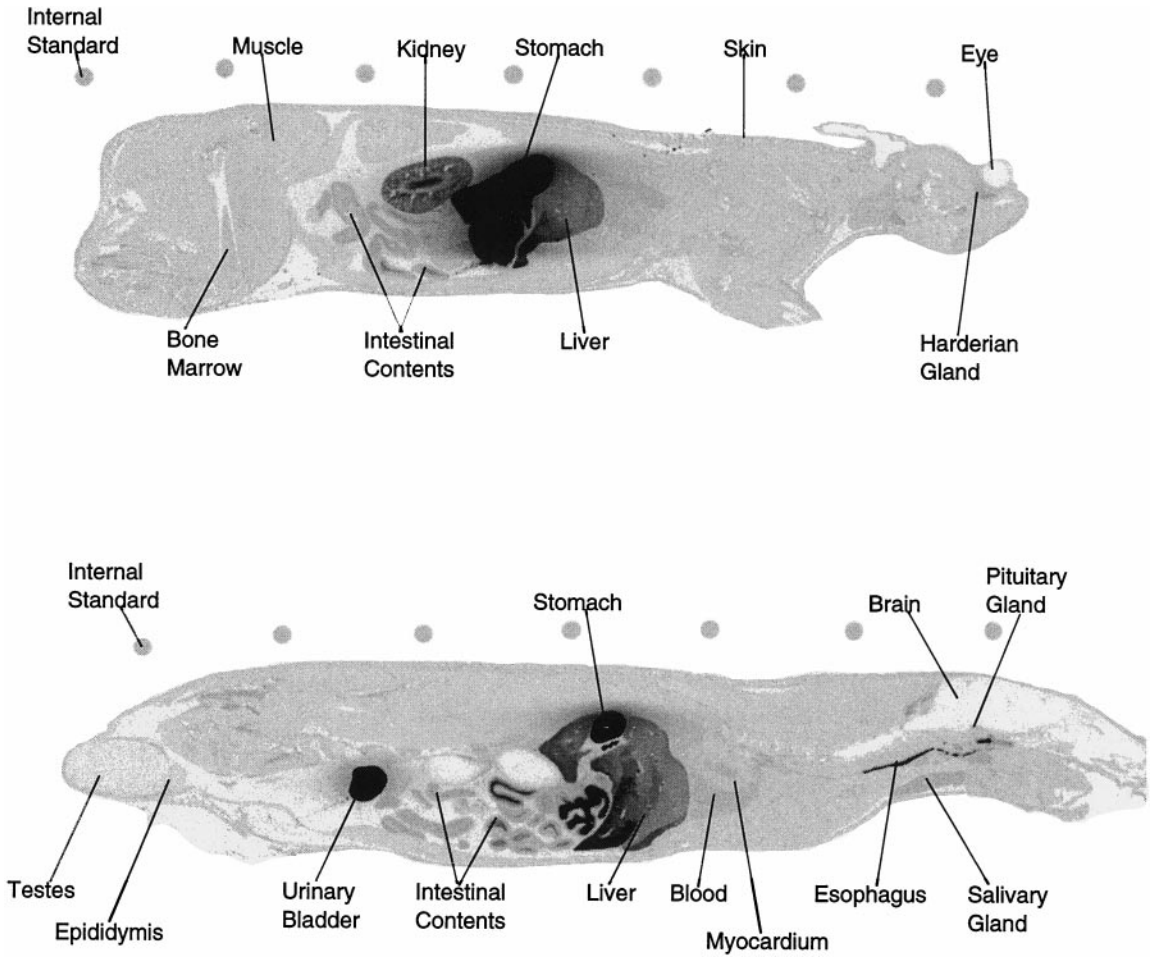

FIG. 9. *Phosphor images of whole body sections from a male F344 rat 1 h after receiving a single oral dose of 5 mg/kg of [^{14}C]moxonidine.*

seems to be a unique metabolite that was only found in vivo in rats, and it was neither detected in other species nor produced with rat liver microsomes or rat liver slices.

In addition to oxidative metabolism, both moxonidine and its metabolites undergo phase II metabolism, forming GSH conjugates and a glucuronide conjugate. Most of the phase II metabolites (G, H, I, J, K, L, M, N, and O) were detected only in bile samples except the glucuronide conjugate of hydroxylated moxonidine, which was detected in both urine and bile samples. An interesting observation during the identification of GSH conjugates is that once the GSH conjugate is formed, it will go through a sequential removal of glutamyl and glycyl moieties to form a cysteinylglycine conjugate and a cysteine conjugate, respectively. Three metabolite pairs (i.e., GSH conjugate/cysteinylglycine conjugate/cysteine conjugate) were identified in bile for each GSH conjugate. The proposed pathways are described as follows. In the presence of GSH, moxonidine is attacked (possibly through SN2 mechanism) and the chlorine moiety is replaced by GSH, generating moxonidine GSH conjugate minus chlorine (metabolite H) and then forming cysteinylglycine conjugate minus chlorine (metabolite K) and cysteine conjugate minus chlorine (metabolite N). The moxonidine GSH conjugate minus chlorine was structurally confirmed by in vitro studies and the cysteine conjugate minus chlorine was structurally confirmed by an authentic standard, both providing supportive evidence for this pathway. The hydroxymethyl moxonidine probably follows the same pathway to form the hydroxymethyl GSH conjugate minus chlorine (metabolite I), then generates the hydroxymethyl cysteinylglycine conjugate minus chlorine (metabolite L) and the hydroxymethyl cysteine conjugate minus chlorine (metabolite O). Additionally, moxonidine forms another GSH conjugate (GSH is located at the imidazolindine ring) in which the chlorine moiety is still attached (metabolite G). This conjugate subsequently produces a cysteinylglycine conjugate (metabolite J) and a glycine conjugate of moxonidine (metabolite M). The mechanism for the formation of metabolite G is unknown. A proposed mechanism involves formation of hydroxy moxonidine (metabolite P, with OH located on the imidazoline ring), which then loses water to form an intermediate with a double bond formed between the carbon atom and the nitrogen atom in the imidazoline ring. Then addition of GSH to the double bound leads to the formation of a GSH conjugate with GSH located at the imidazoline ring (Fig. 8).

Although three different cysteine conjugates (metabolites M, N, and O) have been found in rat bile samples, none of the corresponding mecapturic acid derivatives were detected. It has been reported that the GSH conjugates were synthesized with hepatocytes and secreted preferentially across the canalicular membrane into bile, and were broken down within biliary spaces to form cysteine conjugate. The cysteine conjugate was then reabsorbed by the liver, *N*-acetylated to form mecapturic acid, and re-excreted into bile, completing an intrahepatic pathway for mecapturic acid biosynthesis (Hinchman et al., 1991; Hinchman and Ballatori, 1994). A possible reason for not finding mecapturic acid derivatives in rat bile is because in bile duct-cannulated rats, shunting of the bile into the collection system prevented potential reabsorption of the cysteine conjugates by the liver, therefore preventing the formation of mecapturic acid derivatives.

TABLE 7

Estimated pharmacokinetic parameters from selected tissues in male Fischer 344 rats after a single oral dose of 5-mg/kg of [^{14}C]moxonidine

Tissue	AUC_{0-t}	$AUC_{0-\infty}$	C_{max}	T_{max}	$T_{1/2}$
	μg-Eq · h/g		*μg-Eq/g*	*h*	
Adrenal	1.61	NC	1.17	2	NC
Blood	2.45	NC	1.19	1	NC
Brown Fat	0.49	NC	0.57	2	NC
Epididymis	1.21	NC	0.5	2	NC
Eye	3.23	NC	0.74	2	NC
Harderian Gland	6.11	9.96	1.76	2	3.52
Heart	0.68	NC	0.68	2	NC
Intestinal Wall	3.11	NC	1.34	2	NC
Kidney[a]	128.38	129.34	32.44	2	3.33
Liver[a]	93.48	103.53	20.48	1	20.15
Lung	2.22	2.85	1.09	1	1.46
Lymph Node	0.65	NC	0.7	2	NC
Bone Marrow	0.61	NC	0.66	2	NC
Muscle	0.48	NC	0.56	2	NC
Pancreas	3.41	4.13	1.6	1	1.98
Pituitary Gland	0.91	NC	0.92	2	NC
Preputial Gland	0.75	NC	0.81	2	NC
Prostate Gland	NC	NC	1.3	1	NC
Salivary Gland	4.29	5.24	1.41	2	1.95
Seminal Vesicles	1.01	NC	0.52	2	NC
Skin	0.6	NC	0.67	2	NC
Spleen	NC	NC	0.7	2	NC
Stomach Wall	5.26	6.11	2.81	1	1.76
Testes	0.3	NC	0.41	2	NC
Thymus	0.59	NC	0.68	2	NC
Thyroid Gland	2.37	NC	0.98	2	NC

NC, Not Calculated.
[a] High tissue concentration value from Table 6 used for calculations.

The elimination profiles of radiocarbon were characterized in noncannulated and in bile duct-cannulated rats. Radioactivity was quantitatively recovered in the urine, feces, cage wash, and carcass after oral administration of [^{14}C]moxonidine. Approximately 59% of radioactivity was found in urine and 38% of radioactivity was recovered in feces, indicating that renal excretion was the primary route of radiocarbon elimination. In the study conducted in bile duct-cannulated rats, only about 2% of total radioactivity remained in the feces. The radioactivity recovered in the bile was approximately 33%, which was almost equal to that excreted in the feces from noncannulated rats (38%). These data provide evidence that moxonidine is well absorbed after oral administration and that biliary excretion also played an important role in the elimination of moxonidine. Consistent with the biliary excretion data, both moxonidine and radioactivity showed a second peak at about 4 h after i.v. administration, indicating that moxonidine probably undergoes enterohepatic recirculation. This second peak was not observed after oral administration due to the fact that moxonidine was mostly BQL after 2 h.

The total radioactivity recovery and the urinary radioactivity recovery from the bile duct-cannulated rats were relatively low when compared with that from noncannulated rats. This is probably due to a partial loss of the radioactivity in the bile cannulas tubing or funnels, which were not rinsed after termination of the study, but may have contained bile. Also, Nalge cages rather than stainless steel cages were used for bile duct-cannulated rats. The large surface area of the Nalge cages may allow greater interaction between the cage surface and biological excrements. Some of the urine samples may have dried and remained on the large surface of the cages during the collection and were not rinsed off by water. In addition, it is not known that whether the excretion profiles can be altered due to change of physiological condition in bile duct-cannulated rats or due to collection of bile, preventing the reabsorption of moxonidine and its metabolites from the bile.

The results of the QWBA study demonstrated that radiocarbon associated with [^{14}C]moxonidine and/or its metabolites were widely distributed to tissues with highest levels of radioactivity observed in the kidney and liver. Peak radiocarbon concentrations in most tissues occurred at 1 or 2 h post dose and decreased over time with levels no longer detectable in most tissues at 48 h post dose. Although QWBA accurately determines radiocarbon tissue concentrations and provides data for the calculation of potential radiation exposure, it may not always be robust enough to provide definitive pharmacokinetic parameters in every tissue. The phosphor images obtained from this study indicate that radiocarbon associated with [^{14}C]moxonidine is primarily eliminated through the urine whereas additional low levels are observed in the intestinal contents. Overall in the tissues of F344 rats, the majority of radiocarbon associated with [^{14}C]moxonidine appeared to be eliminated within the first 24 h post dose. These results are consistent with the balance excretion study, which indicated that the radiocarbon was rapidly absorbed and approximately 95% of total radioactivity was eliminated within 24 h post dose primarily by urinary excretion.

All the data gathered from the present studies demonstrate that moxonidine is well absorbed, widely distributed into tissues, and rapidly eliminated in F344 rats after oral administration. The poor bioavailability is caused by extensive first-pass metabolism via both phase I and phase II pathways.

Acknowledgments. We thank Dr. Todd A. Gillespie for valuable discussion on mass spectrometry data, Mark R. Vandenbranden for his assistance in in vitro studies, and Jennifer H. Herman for her technical assistance in QWBA study.

References

Chay SH and Pohland RC (1994) Comparison of quantitative whole-body autoradiographic and tissue dissection techniques in the evaluation of the tissue distribution of [^{14}C]daptomycin in rats. *J Pharm Sci* **83:**1294–1299.

Ernsberger PR, Westbrooks KL, Christen MO and Schafer SG (1992) A second generation of centrally acting antihypertensive agents act on putative I1-imidazoline receptors. *J Cardiol Pharmacol* **20 (Suppl 4):**1–10.

Hinchman CA and Ballatori N (1994) Glutathione conjugation and conversion to mercapturic acid can occur as intrahepatic process. *J Toxicol Environ Health* **41:**387–409.

Hinchman CA, Mastsumoto H, Simmons TW and Ballatori N (1991) Intrahepatic conversion of a glutathione conjugate to its mecapturic acid. Metabolism of 1-chloro-2,4-dinitrobenzene in isolated perfused rat and gunea pig livers. *J Biol Chem* **266:**22179–22185.

Johnston RF, Pickett SC and Barker DL (1990) Autoradiography using storage phosphor technology. *Electrophoresis* **11:**355–360.

Lowry OH, Rosebrough NJ, Farr AL and Randall RJ (1951) Protein measurement with the Folin phenol reagent. *J Biol Chem* **193:**265–275.

Ollivier JP, Christen MO and Schafer SG (1992) Moxonidine, a second generation of centrally acting drugs: An appraisal of clinical experience. *J Cardiol Pharmacol* **20 (Suppl 4):**31–36.

Schaefer HC, Toublanc N and Weihmann HJ (1998) The pharmacokinetics of moxonidine. *Rev Contemp Pharmacother* **9:**481–490.

Ullberg S (1977) The technique of whole body autoradiography: Cryosectioning of large specimens, in *Science Tools*, the LKB instrument journal. Special Issue. pp 2–29.

van der Hoeven TA and Coon MJ (1974) Preparation and properties of partially purified cytochrome P-450 and reduced nicotinamide adenine dinucleotide phosphate-cytochrome P-450 reductase from rabbit liver microsomes. *J Biol Chem* **249:**6302–6310.

Yu A and Frishman WH (1996) Imidazoline receptor agonist drug: A new approach to the treatment of systemic hypertension. *J Clin Pharmacol* **36:**98–111.